

# Nanohole formation in TEOS-HMDSO hybrid CVD films elucidated by positron beams

K Ito, N Oshima, A Yabuuchi and B E O'Rourke

National Institute of Advanced Industrial Science and Technology (AIST), Tsukuba, Ibaraki 305-8565, Japan

E-mail: k-ito@aist.go.jp

**Abstract.** Silicon-oxide-backboned hybrid thin films with thicknesses around 600 nm were fabricated through plasma enhanced chemical vapor deposition from tetraethyl orthosilicate mixed with hexamethyldisiloxane as precursors, and their subnano-scaled holes, generated by annealing at 560 °C, were investigated by means of the positron lifetime technique with a pulsed, low-energy positron beam. The hole dimension was quantified from the *ortho*-positronium lifetime for the as-prepared and annealed films with different compositions. The effect of the heat treatment and the precursor composition on the subnano holes was discussed.

## 1. Introduction

Manufacturing silicon oxide thin films with engineered nanoscaled holes is a key issue for developing various functional materials such as gas sensors [1] and separation membranes [2]. In this work, we fabricated silicon-oxide-backboned thin films with thicknesses of around 600 nm through plasma enhanced chemical vapor deposition (PECVD) from tetraethyl orthosilicate (TEOS) mixed with hexamethyldisiloxane (HMDSO) as precursor of the film, and investigated their nanoscaled holes generated by annealing. By using a pulsed, low-energy positron beam, the hole dimension was quantified from the longest-lived lifetimes of *ortho*-positronium *o*-Ps for the as-prepared and the annealed films with different compositions of the precursors. The effect of the heat treatment and the precursor composition on the nanohole structure is examined in comparison of the positron results with those from Fourier transform infrared spectroscopy and spectroscopic ellipsometry.

## 2. Experimental

Films were deposited on 4-inch silicon wafers at a substrate temperature of 100 °C using a capacitive coupled PECVD reactor with parallel plate electrodes (Fig. 1) [3, 4]. Mixtures of TEOS and HMDSO diluted in argon and oxygen gas were used as precursors. The deposition was carried out under a pressure of 150 Pa with 200 W RF power. The fabricated films were then annealed at 560 °C under dry nitrogen gas flow. The deposition condition, thickness,

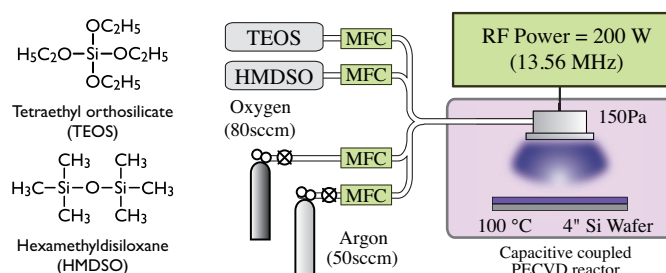


Figure 1: Monomers and PECVD system.



Table 1: Deposition condition (TEOS and HMDSO flow rates, HMDSO feed fraction  $\phi_H$ ), thickness  $L$ , and refractive index  $n$  at 630 nm for the as-deposited and annealed films.

Sample No.	TEOS [sccm]	HMDSO [sccm]	$\phi_H$	As deposited		Annealed	
				$L$ [nm]	$n$	$L$ [nm]	$n$
1	15	0	0	533	1.412	459	1.412
2	9	6	0.4	587	1.417	539	1.406
3	3	12	0.8	578	1.419	585	1.359
4	0	15	1.0	632	1.421	617	1.362

\* $L$  and  $n$  were determined by means of spectroscopic ellipsometry at 26 °C.

and refractive index at 630 nm for the as-deposited and annealed films are listed in Table 1. As in the table, by annealing the respective refractive index  $n$  decreased, especially the higher the HMDSO feed fraction  $\phi_H$ , the lower the refractive index, indicative of the enhanced porosity.

The chemical structure of films was analyzed by Fourier transform infrared (FT-IR) spectroscopy.

Positron annihilation  $\gamma$ -ray energy spectra were measured by using a  $^{22}\text{Na}$ -source-based magnetically-guided beam [5] at positron incident energies  $E$  from 0.01 keV to 25 keV. The line-shape  $S$  parameter, a measure of Doppler broadening of annihilation radiation, was determined as the ratio of the counts appearing in the central region (510.3 keV–511.7 keV) to the total counts around the 511-keV annihilation photo peak (506.8 keV–515.2 keV).

Positron lifetime measurements were carried out by utilizing a  $^{22}\text{Na}$ -based pulsed-positron beam at AIST. Multi-exponential analysis was applied to the recorded lifetime data to deduce the hole radius  $r$  [nm] from the longest-lived  $o$ -Ps lifetime  $\tau$  [ns] based on the following equation [6, 7],

$$\tau = 0.5 \left[ 1 - \frac{r}{r + 0.1656} + \frac{1}{2\pi} \sin\left(\frac{2\pi r}{r + 0.1656}\right) \right]^{-1} \quad (1)$$

### 3. Results and discussion

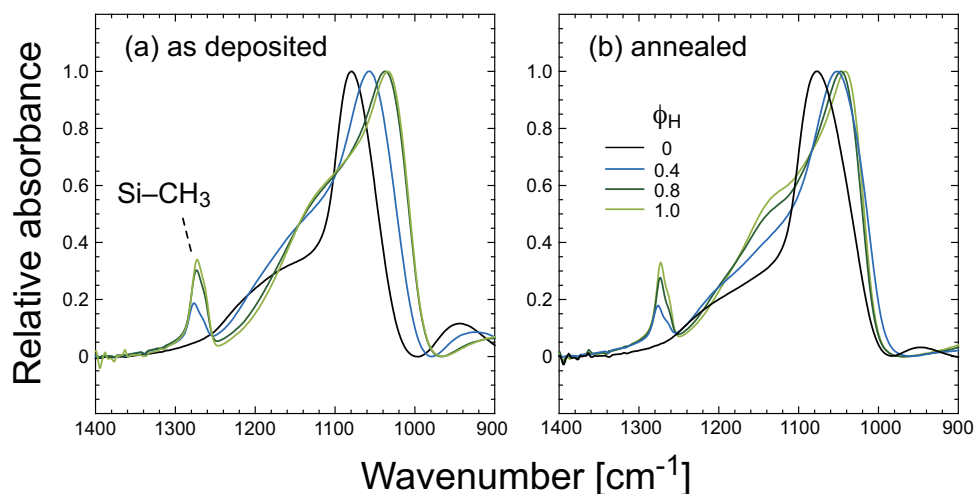


Figure 2: FT-IR spectra for the present PECVD films; (a) as-deposited films, (b) annealed films.

Figure 2 shows the FT-IR spectra for the PECVD films before and after annealing. The distinct absorption peak around  $1100 \text{ cm}^{-1}$  for the film with  $\phi_H = 0$  is due to the Si-O-Si stretching mode [8].

With increasing  $\phi_H = 0$  the peak for both the as-deposited and annealed films is shifted to the lower wavenumber, indicative of the enhanced absorption relevant to C–Si–O bonds in the silica network [9]. The absorption intensity for the peak around  $1280\text{ cm}^{-1}$ , ascribable to Si–CH<sub>3</sub> stretching, increases with increasing  $\phi_H$ , signifying the increased number of the terminal CH<sub>3</sub> in the network structure.

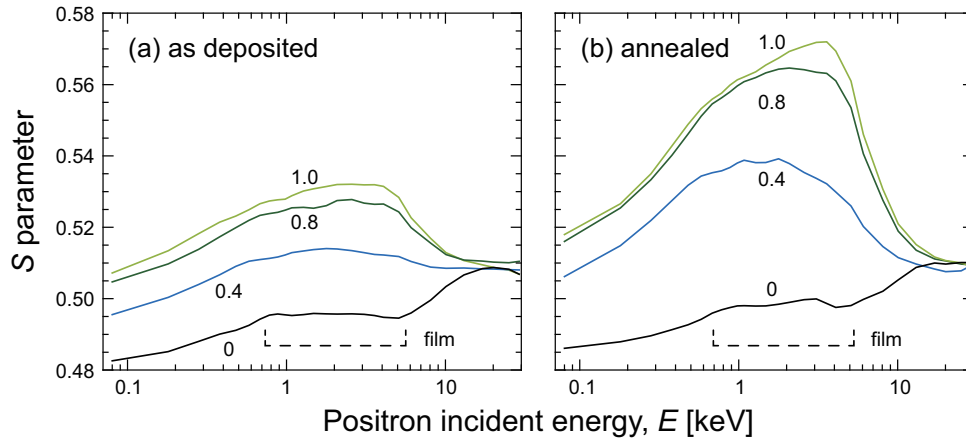


Figure 3:  $S$ – $E$  curve for the as-deposited films (a) and the annealed films at  $560\text{ }^\circ\text{C}$  (b). The values represent the HMDSO feed fraction  $\phi_H$ .

Figure 3 shows the variation of the line-shape  $S$  parameter for the present samples as a function of positron incident energy  $E$  ( $S$ – $E$  curve). The  $S$ – $E$  curve is divided roughly into four stages, namely, (1)  $E < 0.7\text{ keV}$ , (2)  $0.7\text{ keV} \lesssim E < 5.5\text{ keV}$ , (3)  $5.5\text{ keV} \lesssim E < 15\text{ keV}$ , and (4)  $15\text{ keV} \lesssim E$ , and those are reasonably ascribed to the annihilation of positrons (1) in the film subsurface region, (2) in the film, (3) in the interface region between the film and the silicon substrate, and (4) in the silicon substrate, respectively. For the as-deposited films the  $S$  value at  $0.7\text{ keV} \lesssim E < 5.5\text{ keV}$  increases with increasing  $\phi_H$  as in Fig. 3(a). On the other hand, for the annealed films (Fig. 3(b)) although the tendency of  $S$  on  $\phi_H$  is similar, the variation with  $\phi_H$  is more enhanced, probably due to the increased Ps formation with the increased film porosity after annealing at  $560\text{ }^\circ\text{C}$  and/or due to the specific annihilation of positrons with the terminal CH<sub>3</sub> groups on the hole surface, leading to higher  $S$  value [10].

Figure 4 shows the positron lifetime data obtained at  $E = 3.0\text{ keV}$  for the as-deposited and annealed films. The lifetime data for the films annealed at  $560\text{ }^\circ\text{C}$  have the longer lifetimes than for the respective as-deposited films. This suggests that larger holes are introduced, possibly as a result of the decomposition of ‘unreacted’ components in the as-deposited films by annealing. Table 2 lists the analyzed longest-lived  $o$ -Ps lifetimes  $\tau$ , their relative intensities  $I$ , and hole radii  $r$ , obtained from the respective  $\tau$ , for the as-deposited and annealed films. As in the table,  $\tau$  for the as-deposited films ranges from  $2.6\text{ ns}$  to  $3.5\text{ ns}$ , slightly increases with increasing  $\phi_H$ . By annealing each  $\tau$  increases, as a result, it ranges from  $2.9\text{ ns}$  to  $8.6\text{ ns}$ , indicating that the larger holes, ranging from  $0.36\text{ nm}$  to  $0.61\text{ nm}$  in radius, are formed in the films with the higher  $\phi_H$  by annealing. This may be relevant to the enhanced  $S$  by the annihilation of positrons with the terminal hydrocarbon groups at the hole surface in addition to the slight increase of  $I$ .

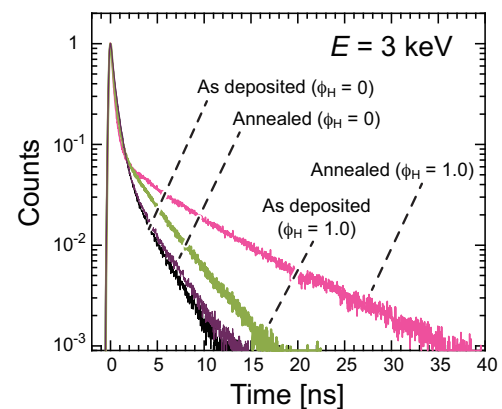


Figure 4: Typical positron annihilation lifetime data (corrected for the background).

Table 2: Longest-lived *o*-Ps lifetimes  $\tau$ , their relative intensities  $I$  and hole radii  $r$  obtained from  $\tau$  for the as-deposited and annealed films. The values in the parenthesis represent the respective standard deviation on the analysis.

Sample No.	$\phi_H$	As deposited			Annealed		
		$\tau$ [ns]	$r$ [nm]	$I$ [%]	$\tau$ [ns]	$r$ [nm]	$I$ [%]
1	0	2.67 (0.009)	0.344	22.5 (0.1)	2.91 (0.009)	0.360	24.5 (0.1)
2	0.4	3.34 (0.007)	0.388	35.9 (0.1)	4.44 (0.009)	0.448	40.5 (0.1)
3	0.8	3.43 (0.007)	0.393	39.4 (0.1)	7.57 (0.220)	0.576	46.8 (0.2)
4	1.0	3.48 (0.007)	0.396	41.1 (0.1)	8.62 (0.004)	0.612	45.2 (0.3)

#### 4. Conclusion

We have investigated nanopore formation upon heat treatment for TEOS–HMDSO hybrid PECVD films by means of the variable-energy positron annihilation  $\gamma$ -ray and lifetime techniques. The IR and ellipsometry results clearly indicated that the absorption intensity for the Si–CH<sub>3</sub> bond is enhanced with increased HMDSO feed fraction  $\phi_H$ , while the refractive index after annealing is reduced, suggesting increased porosity. The positron lifetime results demonstrated that the larger holes are formed in the annealed films, signifying that subnanoscopic hole size up to 0.6 nm in radius for the TEOS–HMDSO hybrid system is tunable with the precursor composition at deposition in combination with pyrolysis.

#### Acknowledgments

This work was supported by a Grant-in-Aid for Scientific Research (24246126) from JSPS, Japan. KI thanks Dr. Hideaki Hagihara of AIST for his assistance to the lifetime measurements.

#### References

- [1] Guizard C, Bac A, Barboiu M, and Hovnanian N 2001 *Sep. Purif. Technol.* **25** 167–180
- [2] Wang J, Gong G, Kanezashi M, Yoshioka T, Ito K, Tsuru T 2013 *J. Membrane Sci.* **441** 120–128
- [3] Oka T, Ito K, Muramatsu M, Ohdaira T, Suzuki R, and Kobayashi Y 2006 *J. Phys. Chem. B* **110** 20172
- [4] Ito K, Oka T, Kobayashi Y, Suzuki R, and Ohdaira T 2007 *Radiat. Phys. Chem.* **76** 213–216
- [5] Kobayashi Y, Kojima I, Hishita S, Suzuki T, Asari E, and Kitajima M 1995 *Phys. Rev. B* **52** 823–828
- [6] Tao S J 1972 *J. Chem. Phys.* **56** 5499–5510
- [7] Eldrup M, Lightbody D, and Sherwood J N 1981 *Chem. Phys.* **63** 51–58
- [8] Tripp C P and Hair M L 1991 *Langmuir* **7** 923–927
- [9] Morent R, Geyter N D, Vlierberghe S V, Dubruel P, Leys C, Schacht E 2009 *Surf. Coat. Tech.* **203** 1366–1372
- [10] Sato K, Ito K, Hirata K, Yu R S, and Kobayashi Y 2005 *Phys. Rev. B* **71** 012201